

## Recoil-implanted $^{57}\text{Fe}$ in diamond

K. Bharuth-Ram

*Physics Department, University of Durban-Westville, Durban 4000, South Africa*

M. Hartick, E. Kankeleit, C. Dorn, and P. Held

*Institut für Kernphysik, Technische Hochschule-Darmstadt, D-62489 Darmstadt, Germany*

R. Sielemann and L. Wende

*Hahn-Meitner-Institut, Glienickerstrasse 100, D-14109 Berlin, Germany*

J. Kübler

*Institut für Kernphysik, Technische Hochschule-Darmstadt, D-62489 Darmstadt, Germany*

J. P. F. Sellschop

*University of the Witwatersrand, P.O. WITS, 2050 Johannesburg, South Africa*

(Received 10 April 1998)

The lattice sites of  $^{57}\text{Fe}$  recoil implanted into diamond at low concentrations have been investigated in in-beam Mössbauer spectroscopy.  $^{40}\text{Ar}$  ions incident at 110 MeV on an enriched  $^{57}\text{Fe}$  foil were used to Coulomb excite and recoil implant  $^{57}\text{Fe}$  nuclei into a pair of diamond targets. Conversion electron Mössbauer spectra were measured at sample temperatures of 300, 600, 700, and 800 K. The spectra were consistently resolved into three components: two symmetric doublets and a weak singlet. At 300 K the singlet had an isomer shift of  $\delta = +0.16$  mm/s; the doublets ( $D_1$  and  $D_2$ ) had quadrupole splittings of 2.33 mm/s and 2.10 mm/s, and isomer shifts of  $-0.51$  mm/s and  $+0.04$  mm/s, respectively. The line intensities and linewidths of the three components showed little change with temperature. Time-differential measurements showed no evidence of any dynamic rearrangement of the implanted Fe atoms within the time window of the measurements (100 ns). Comparison of the observed isomer shifts with theoretical calculations and similar measurements in Si allow us to attribute the singlet ( $f \approx 10\%$ ) to interstitial Fe. The isomer shift of doublet  $D_2$  is in agreement with the calculations for substitutional Fe. However, the large electric-field gradients of  $D_1$  and  $D_2$  caution against any firm conclusions on these components, but indicate that two differently disturbed implantation sites are populated with considerable lattice damage in the neighborhood of the implanted ions. [S0163-1829(98)02237-1]

### I. INTRODUCTION

Ion implantation has found increasing application in recent years as a means of incorporating dopant atoms in semiconductors, especially in systems where solubility of the dopant atoms is low. Diamond is one such system, where the extremely low solubility of potential  $n$ -type dopants rule out thermal diffusion or incorporation during growth as doping mechanisms. Ion implantation is an attractive alternative, and has been used in several recent studies on diamond.<sup>1-5</sup> Ion implantation is free of any limitations imposed by solubility considerations and offers precise control of dopant species, depth, and concentration. However, a major difficulty is that the implantation process is invariably accompanied by lattice damage, which is compounded in semiconductors by the large variety of defects that can be formed. Hence, several techniques, and in particular, Mössbauer spectroscopy,<sup>6-10</sup> have been used to investigate the implantation sites and diffusion of dopant atoms in diamond, and to study the immediate neighborhood of the implanted atoms and their annealing characteristics.

The resonance spectra observed in the early Mössbauer studies were characterized by a broad doublet. Sawicka,

and de Waard,<sup>7-9</sup> in investigations on  $^{57}\text{Co}$  implanted into diamond, obtained spectra dominated by a broad doublet that suggested that the majority of the implanted Fe atoms were in highly damaged regions in the host matrix. A weak singlet component was also observed whose intensity increased from 3% at 300 K to 20% at annealing temperatures above 600 K, indicating a transition of the implanted atoms to a high-symmetry site. A systematic study of the amorphization of the diamond lattice produced by the implantation of different doses of  $^{57}\text{Co}$  was conducted by de Potter and Langouche.<sup>10</sup> Their data showed that implantation doses  $\geq 10^{15}$  Co cm<sup>-2</sup> results in the formation of a completely amorphous layer, which does not anneal up to temperatures of 1173 K, and that the isomer shifts of some components were dependent on the implantation dose. Mössbauer spectra obtained for a dose of  $10^{14}$  cm<sup>-2</sup> were resolved into two doublets and two singlets. The singlets had quite large isomer shifts, indicative of the considerable lattice strain around the Fe atoms.

Very little information exists on lattice location of Fe atoms implanted in diamond. Molecular-orbital calculations by Lowther<sup>11</sup> suggest that Fe should be stable in substitutional and metastable in interstitial sites. The present measurements

were therefore aimed at investigating the lattice sites of Fe atoms in diamond achieved with low dose implantation, and were therefore undertaken employing the in-beam Mössbauer spectroscopy (IBMS) technique, and exploiting some of its unique features.<sup>12</sup> In the IBMS method, Coulomb excitation reactions of a heavy-ion beam (Ar or Xe) on an enriched  $^{57}\text{Fe}$  foil result in electric quadrupole ( $E2$ ) excitations of the  $\frac{3}{2}^-$  and  $\frac{5}{2}^-$  states in  $^{57}\text{Fe}$  at 136, 366, and 706 keV. Close to 90% of the population of these states decay into the Mössbauer level at 14.4 keV. The excited  $^{57}\text{Fe}^*$  nuclei leave the foil with their angular distribution peaked between  $20^\circ$  and  $70^\circ$ , and therefore may be implanted into samples mounted on either side of the beam axis, while the primary beam passes through without striking the samples. The kinetic energy imparted to the recoiling nuclei ranges up to several MeV, and results in a uniform implantation profile with a depth extending to  $10\ \mu\text{m}$ . The sample, implanted with the excited  $^{57}\text{Fe}^*$  nuclei, acts as a source, and, hence, low implantation doses ( $\leq 10^{11}\ \text{cm}^{-2}$ ) are sufficient to obtain spectra with good statistics. This coupled with the large implantation range results in extremely low dopant concentrations ( $\leq 10^{15}\ \text{cm}^{-3}$ ). Single atom implantation is thus achieved, there is no interaction between neighboring probe atoms, and overlap of implantation induced damage cascades is avoided. Recoilless emission of the 14.4 keV  $\gamma$  rays from  $^{57}\text{Fe}$  occurs within the lifetime ( $\tau = 141\ \text{ns}$ ) of the Mössbauer state after the implanted probes have come to rest. Hence, the probes cannot form clusters, precipitate, or escape from the sample during the time window of the measurement. However, one drawback of the IBMS technique is that the measurements are performed in the ‘as-implanted’ state at the sample temperature. Thermal treatment of the host sample, such as an isochronal annealing sequence, is not possible.

## II. EXPERIMENTAL

The measurements were made at the VICKSI accelerator at the Hahn-Meitner-Institute, Berlin. The  $^{57}\text{Fe}$  nuclei were produced in their 14.4 keV Mössbauer state by bombarding an enriched  $^{57}\text{Fe}$  foil with a pulsed 110 MeV  $^{40}\text{Ar}$  beam. The Fe foil was  $2\ \text{mg}/\text{cm}^2$  thick and covered with a  $100\ \mu\text{g}/\text{cm}^2$  layer of Ag for thermal conduction. It was kept at liquid nitrogen temperature during measurements. The  $^{40}\text{Ar}$  beam, of intensity 150 nA, had a pulse width of 2 ns and a repetition period of 400 ns and was swept vertically over the Fe target at a frequency of 200 Hz. To reduce background data was collected only during beam-off period.

Details of the IBMS arrangement are given in Ref. 13. Diamond targets of large surface area ( $20\ \text{mm} \times 20\ \text{mm}$ ) were required. Hence, each target was assembled from  $5.0\ \text{mm} \times 5.0\ \text{mm} \times 2\ \text{mm}$  thick ‘tiles’ of synthetic high-temperature high-pressure produced type-Ib single-crystal diamonds, with the nitrogen concentration kept below 100 ppm. The ‘tiles’ were polished parallel to the (100) faces, carefully aligned and brazed onto a metal backing plate. A pair of halogen lamps mounted behind the samples allowed controlled heating of the samples up to a temperature of 900 K. Two diamond targets were used, mounted on either side of the primary beam. This arrangement allowed the recoiling  $^{57}\text{Fe}^*$  nuclei to be implanted into the target samples while the  $^{40}\text{Ar}$  beam passed through without striking the samples.

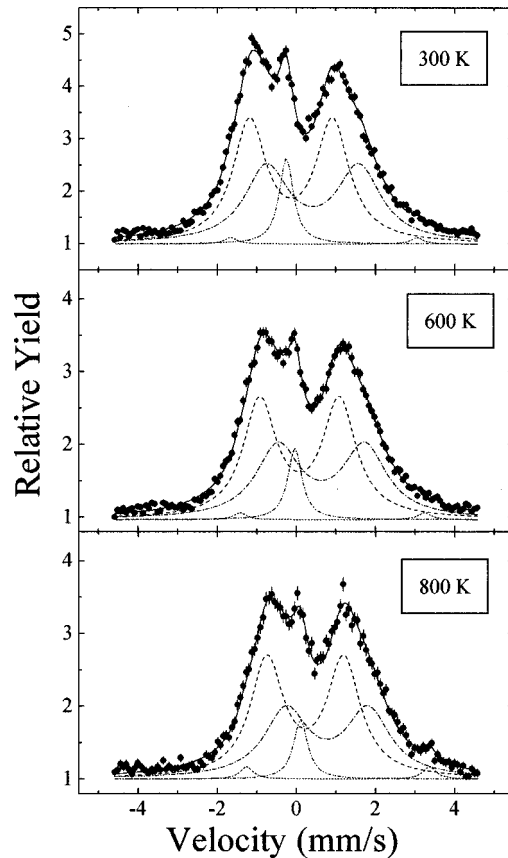


FIG. 1. In-beam Mössbauer spectra of Fe in diamond. The spectra were consistently resolved into a singlet and two doublets.

Because of the special construction of the targets the Mössbauer measurements were made in reflection geometry. Conversion electron spectra of the 14.4 keV  $\gamma$  quanta were collected with small, light-weight resonance counters mounted directly onto conventional Mössbauer drives that were operated in constant acceleration mode. The resonance counters were gas-filled parallel plate avalanche counters, with one electrode made of stainless steel foil in which the Fe content was enriched to 95% in  $^{57}\text{Fe}$  (Ref. 14). Spectra were collected in time-differential mode<sup>15</sup> for sample temperatures of 300, 600, 700, and 800 K.

## III. RESULTS

Mössbauer spectra for sample temperatures of 300, 600, and 800 K are displayed in Fig. 1. The spectra have the overall shape of broad symmetric doublets together with a weak singlet, and show little change with temperature. To obtain consistent fits the spectra were analyzed in several different ways. An initial analysis, in which the spectra were fitted with a single broad doublet and a singlet, as was found for similar IBMS measurements in Si,<sup>16</sup> failed to produce satisfactory fits to the data. The most consistent results were obtained in an analysis in which the spectra at the four temperatures were fitted simultaneously, allowing for the expected second-order Doppler shift in isomer shift with sample temperature. Such a fit required two symmetric doublets,  $D_1$  and  $D_2$ , and a singlet  $S_1$ . The parameters extracted from the analysis are listed in Table I, where the isomer shifts are expressed as absorber shifts relative to  $\alpha\text{-Fe}$ .

TABLE I. Linewidth  $\Gamma$  (FWHM), isomer shift ( $\delta$ ), quadrupole splitting ( $\Delta E_Q$ ), and line area ( $A$ ), of the singlet ( $S_1$ ) and doublets ( $D_1$  and  $D_2$ ) observed in the resonance spectra at the different sample temperatures. The isomer shifts are expressed as absorber shifts relative to  $\alpha\text{-Fe}$ .

Temp. (K)	$D_1$ ( $\Gamma = 1.3$ mm/s)			$D_2$ ( $\Gamma = 1.0$ mm/s)			$S_1$ ( $\Gamma = 0.5$ mm/s)	
	$\delta$ (mm/s)	$\Delta E_Q$ (mm/s)	$A$ (%)	$\delta$ (mm/s)	$\Delta E_Q$ (mm/s)	$A$ (%)	$\delta$ (mm/s)	$A$ (%)
300	-0.51(3)	2.33(3)	42(2)	+0.04(3)	2.10(3)	50(2)	+0.16(5)	8(1)
600	-0.73(3)	2.19(3)	41(2)	-0.18(3)	2.01(3)	51(2)	-0.12(5)	8(1)
700	-0.80(3)	2.13(3)	41(2)	-0.25(3)	1.98(3)	52(2)	-0.13(5)	7(1)
800	-0.89(3)	2.07(3)	40(2)	-0.33(3)	1.94(3)	52(2)	-0.20(5)	7(1)

A 300 K, the quadrupole splittings  $\Delta E_Q$  of the doublets were 2.33(5) mm/s and 2.10(5) mm/s, respectively, corresponding to electric-field gradients  $V_{zz}$  of  $1.07 \times 10^{18}$  V/cm<sup>2</sup> and  $0.96 \times 10^{18}$  V/cm<sup>2</sup>. These values are quite large, but consistent with the electric-field gradients observed for other heavy ions in diamond.<sup>17</sup> The quadrupole splittings decrease with increasing temperature, following a  $T^{3/2}$  dependence, as is shown in Fig. 2, with proportionality constants  $-1.50(2) \times 10^{-2} \text{ K}^{-3/2}$  and  $-0.91(2) \times 10^{-2} \text{ K}^{-3/2}$  for doublets  $D_1$  and  $D_2$ , respectively.

A search was made for evidence of dynamic rearrangement of the  $^{57}\text{Fe}$  probe atoms between implantation and decay, by binning the time differential spectra into four time bins of 50–125, 125–200, 200–275, and 275–350 ns. Spectra measured at 300 K are shown in Fig. 3. Little evidence of any temporal behavior is evident. Dynamic rearrangements, if any, occur within a time  $\leq 100$  ns after implantation.

#### IV. DISCUSSION

In Table II we compare the isomer shifts and quadrupole splittings determined in our measurements with the results of de Potter and Langouche<sup>10</sup> and Sawicka, Sawicki, and de Waard.<sup>7</sup> The earlier results were obtained from measurements in which  $^{57}\text{Co}$  was implanted into diamond samples at energies of 85 and 50 keV, respectively, and at implantation doses of  $10^{14} \text{ cm}^{-2}$  and  $5 \times 10^{13} \text{ cm}^{-2}$ . The isomer shifts of the doublets are in reasonable agreement with those observed

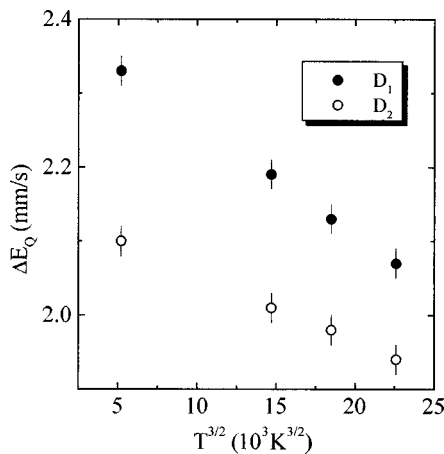


FIG. 2. Quadrupole splitting  $\Delta E_Q$  of doublets  $D_1$  and  $D_2$  plotted as a function of  $T^{3/2}$ .

in Ref. 10. The spectra in Ref. 7 were fitted with a singlet and a single broad doublet; the isomer shift of the doublet is in reasonable agreement with the mean shift of the two components required to fit our data. The values of the quadrupole splittings are a little smaller than observed in the earlier measurements, which may be reflecting the reduced damage produced in the vicinity of the probes in the present low dose in-beam measurements.

The singlet  $S_1$  in our data has an isomer shift  $\delta = +0.16$  mm/s. Singlet components with large negative isomer shifts, as were observed previously, were not evident in our spectra. Two sources could contribute to the different results. The first is the large difference in the dopant concentration

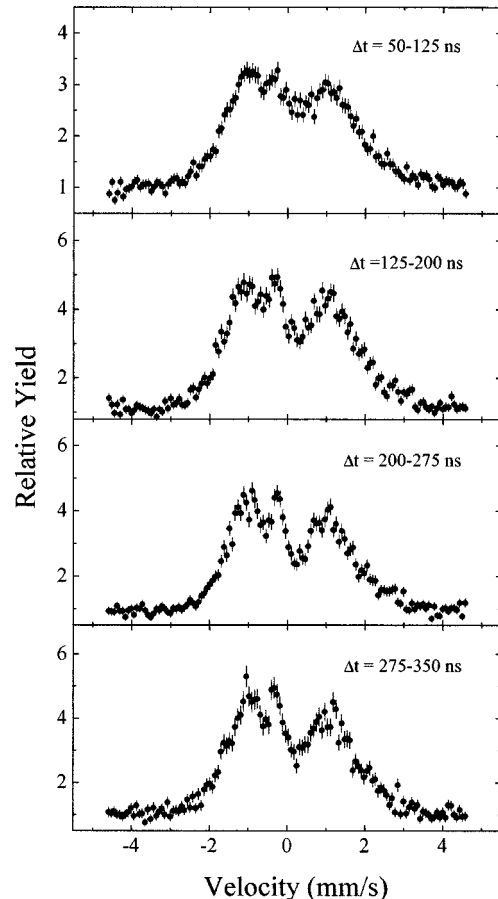


FIG. 3. Time-differential Mössbauer spectra of Fe in diamond observed at 300 K, for time intervals 50–125, 125–200, 200–275, and 275–350 ns, after implantation.

TABLE II. Isomer shifts ( $\delta$ ) and quadrupole splittings ( $\Delta E_Q$ ) of the singlet ( $S_i$ ) and doublets ( $D_i$ ) determined in the present measurements compared with the results of de Potter and Langouche (Ref. 10) and Sawicka, Sawicki, and de Waard (Ref. 7). The isomer shifts are expressed as absorber shifts relative to  $\alpha$ -Fe.

Component	Present	Ref. 10	Ref. 7
$D_1$ : $\delta$ (mm/s)	-0.51(3)	-0.70(5)	
$\Delta E_Q$ (mm/s)	2.33(3)	2.60(5)	
$D_2$ : $\delta$ (mm/s)	+0.04(3)	-0.16(5)	-0.12(5)
$\Delta E_Q$ (mm/s)	2.10(3)	2.47(5)	2.3(1)
$S_1$ : $\delta$ (mm/s)	+0.16(5)	+1.61(5)	
$S_2$ : $\delta$ (mm/s)		-0.79(5)	-0.95(5)

which is less by a factor of  $10^5$  in our IBMS measurements compared with those used in Refs. 7–10. The single line components with large negative isomer shifts observed in the earlier measurements have been attributed to probes at regular but highly compressed lattice sites. Evidently these forces are reduced in the IBMS measurements. A second factor is that in our case excited  $^{57}\text{Fe}$  probes are directly implanted into the host whereas in the source based measurements radioactive  $^{57}\text{Co}$  were implanted in the diamond samples. Aftereffects of the  $^{57}\text{Co} \rightarrow ^{57}\text{Fe}$  electron capture decay may make some contribution to the difference in the electron charge distribution around the probes.

In order to identify the implantation sites of the Fe atoms theoretical calculations were made of the contact charge densities at the Fe nuclei at substitutional ( $S$ ) and tetrahedral interstitial ( $T$ ) sites. The calculations were carried out in exactly the same way as for earlier calculations for Fe in Si and Ge,<sup>18</sup> i.e., they were made within the local-density approximation of spin-density-functional theory (LSDA), and used the augmented nonrelativistic spherical wave method to solve effective single-particle wave equations self-consistently. The Fe configurations were simulated by placing Fe in a large supercell that was then periodically repeated. For an interstitial lattice position, one Fe atom was placed at the origin and the surrounding diamond lattice filled with sixteen C atoms. For a substitutional defect, the diamond lattice along each of the three unit-cell edges was doubled and the central C atom replaced with a Fe atom. The supercell for the  $T$  and  $S$  configurations may be represented as  $\text{FeC}_{16}E_{15}$  and  $\text{FeC}_{15}E_{16}$ , respectively, where  $E$  represents the interstitial (“empty”) sphere. Self-consistent wavefunctions were generated for Fe at the two configurations in diamond and in  $\alpha$ -Fe, and the contact charge densities at the Fe nucleus were calculated with non-relativistic corrections.

For Fe atoms at tetrahedral interstitial sites the calculations gave a contact charge density, relative to  $\alpha$ -Fe, of  $\Delta\rho = -0.623a_0^{-3}$ , i.e., a reduced electron density at the Fe nucleus, which corresponds to an isomer shift of  $\Delta S = +0.22$  mm/s. For substitutional Fe, the results depend on the relaxation of the Fe-C bond. In an unrelaxed lattice, the calculations give an increased relative contact charge density of  $\Delta\rho = +0.55a_0^{-3}$ , and a corresponding isomer shift of  $\Delta S = -0.19$  mm/s. Allowing for a small relaxation of the Fe-C separation reduces the relative contact charge density to  $\Delta\rho = -0.26a_0^{-3}$ , and results in an isomer shift of  $+0.09$  mm/s.

In order to interpret our results we compare, in Table III,

TABLE III. Comparison of experimental and calculated isomer shifts of  $^{57}\text{Fe}$  in diamond and Si. The isomer shifts (in mm/s) are expressed as absorber shifts relative to  $\alpha$ -Fe.

	Expt.	Theory	
		Interstitial	Substitutional
(a) Diamond	$D_1$ : -0.51(3)	+0.22	+0.09–-0.19
	$D_2$ : +0.04(3)		
	$S_1$ : +0.16(5)		
(b) Si	$D$ : +0.10(3)	+0.89	+0.13
(Refs. 16 and 18)	$S_1$ : +0.75(5)		
	$S_2$ : -0.20(5)		

our experimental and calculated isomer shifts for Fe in diamond, with results for Si.<sup>16,18</sup> The IBMS spectra in Si show one strong doublet ( $f \approx 70\%$ ) and a singlet ( $f \approx 30\%$ ). LSDA calculations identical to those carried out in the present case reproduce the observed isomer shifts very well<sup>18</sup> and indicate that in Si the singlet ( $S_1$ ) with  $\delta = +0.75$  mm/s is due to tetrahedral interstitial Fe, while a second singlet that appears at temperatures  $T \geq 600$  K may be attributed to substitutional Fe. The observed diffusional broadening of component  $S_1$  confirms this assignment.<sup>16</sup> This gives confidence in the present calculations and allows us to interpret the singlet component ( $f = 10\%$ ) as due to Fe implanted at highly symmetric tetrahedral interstitial sites in diamond. Up to a sample temperature of 800 K this component shows no increase in intensity or in linewidth.

The isomer shift of doublet  $D_2$  ( $= +0.04$  mm/s) is in good agreement with that calculated for substitutional Fe with a relaxed Fe-C bond length. This agreement, however, may be fortuitous. The atomic radii of carbon and iron atoms are 0.77 and 1.26 Å, respectively, and so the Fe environment should be strongly perturbed and result in a large quadrupole splitting, as is observed. Also arguing against assigning  $D_2$  to substitutional Fe is the fact that in all cases where Fe is not soluble in metals and in Si little or no substitutional component is observed immediately after implantation. Examination of the Si IBMS results<sup>18</sup> shows that the substitutional component appears only at high temperatures, presumably due to part of the defect doublet transforming into the substitutional component through Fe interaction with vacancies close to the defect. In diamond, with its Debye temperature  $\approx 2000$  K, such a process is expected to occur at very much higher temperatures. Indeed, emission channeling and perturbed angular correlation measurements on As and In ions implanted in diamond<sup>19</sup> show that large substitutional fractions of dopants in diamond require either implantation or annealing at temperatures above 1200 K. These measurements also show that the majority of the implanted heavy ions are at highly damaged lattice sites that do not recrystallize even at temperatures above 1600 K.

The present measurements were carried out on synthetic type-Ib diamond which contained 100 ppm nitrogen (concentration  $= 1.7 \times 10^{17} \text{ cm}^{-3}$ ) at single substitutional sites. The substitutional  $N$  could present trapping points for the Fe ions. However, the resonance structure observed in our spectra is similar to that observed in natural type-II diamonds (Refs. 7–10), and suggest that the more likely cause of the doublet components is lattice damage due to the mis-

match of both the Fe/C atomic radii and masses.

Doublets  $D_1$  and  $D_2$  represent  $\approx 40\%$  and  $50\%$ , respectively, of the total resonance area in our spectra. Neglecting effects due to different recoil-free fractions, our results then indicate that we implant approximately 10% of the Fe into interstitial sites, and the rest in two differently disturbed, but strongly perturbed sites.

## V. CONCLUSIONS

We have performed in-beam Mössbauer measurements on  $^{57}\text{Fe}$  Coulomb excited and implanted in diamond at temperatures up to 800 K. Comparison of our results with similar

measurements in Si and with theoretical calculations indicate that approximately 10% of the Fe ions are implanted at highly symmetric, tetrahedral interstitial sites. The remainder of the ions reside in two differently perturbed, but strongly damaged environments, where they experience very large electric field gradients ( $\approx 1.0 \times 10^{18}$  V/cm).

## ACKNOWLEDGMENTS

We thank De Beers Industrial Diamonds (Pty) Ltd. who supplied the diamonds, and M. Rebak for the expert construction of the target.

- 
- <sup>1</sup>G. Braunstein and R. Kalish, *J. Appl. Phys.* **54**, 2106 (1983).  
<sup>2</sup>G. Braunstein and R. Kalish, *Nucl. Instrum. Methods* **182/183**, 691 (1981).  
<sup>3</sup>M. Restle, K. Bharuth-Ram, H. Quintel, C. Ronning, U. Wahl, H. Hofsäss, and S. G. Jahn, *Appl. Phys. Lett.* **66**, 2733 (1995).  
<sup>4</sup>K. Bharuth-Ram, H. Quintel, M. Restle, C. Ronning, H. Hofsäss, and S. G. Jahn, *J. Appl. Phys.* **78**, 5180 (1995).  
<sup>5</sup>H. Quintel, K. Bharuth-Ram, M. Restle, C. Ronning, and H. Hofsäss, *Nucl. Instrum. Methods Phys. Res. B* **118**, 72 (1996).  
<sup>6</sup>G. L. Latshaw, P. B. Russell, and S. S. Hanna, *Hyperfine Interact.* **8**, 105 (1980).  
<sup>7</sup>B. D. Sawicka, J. A. Sawicki, and H. de Waard, *Phys. Lett.* **85A**, 303 (1981).  
<sup>8</sup>J. A. Sawicki and B. D. Sawicka, *Nucl. Instrum. Methods Phys. Res.* **194**, 465 (1982).  
<sup>9</sup>J. A. Sawicki and B. D. Sawicka, *Nucl. Instrum. Methods Phys. Res. B* **46**, 38 (1990).  
<sup>10</sup>M. de Potter and G. Langouche, *Z. Phys. B* **53**, 89 (1983).  
<sup>11</sup>J. E. Lowther, *Phys. Lett.* **104A**, 273 (1984).  
<sup>12</sup>R. Sielemann, *Hyperfine Interact.* **80**, 1239 (1993).  
<sup>13</sup>P. Schwalbach, in *Proceedings of the XXIV Zakopane School on Physics*, edited by J. Stanek and A. T. Pedziwiatr (World Scientific, Singapore, 1990).  
<sup>14</sup>G. Weyer, *Mössbauer Effect Meth.* **3**, 301 (1973).  
<sup>15</sup>S. Laubach, P. Schwalbach, M. Hartick, E. Kankeleit, B. Keck, M. Menningen, and R. Sielemann, *Z. Phys. B* **75**, 173 (1989).  
<sup>16</sup>P. Schwalbach, S. Laubach, M. Hartick, E. Kankeleit, B. Keck, M. Menningen, and R. Sielemann, *Phys. Rev. Lett.* **64**, 1274 (1990).  
<sup>17</sup>J. P. F. Sellschop, S. H. Connell, K. Bharuth-Ram, H. Appel, E. Sideras-Haddad, and M. C. Stemmett, *Mater. Sci. Eng., B* **11**, 227 (1992).  
<sup>18</sup>J. Kübler, A. E. Kumm, H. Overhof, P. Schwalbach, M. Hartick, E. Kankeleit, B. Keck, L. Wende, and R. Sielemann, *Z. Phys. B* **92**, 155 (1993).  
<sup>19</sup>K. Bharuth-Ram, A. Burchard, M. Deicher, K. Freitag, H. Hofsäss, S. G. Jahn, R. Magerle, H. Quintel, M. Restle, and C. Ronning, *Hyperfine Interact. C* **1**, 411 (1996).